Scaling Laws for the Slumping of a Bingham Plastic Fluid

Lydie Staron

CNRS - Université Pierre et Marie Curie Paris 6, UMR 7190, Institut Le Rond d'Alembert, F-75252 Paris, France.

School of Earth Sciences, University of Bristol, Queens Road, Bristol BR8 1RJ, United Kingdom

Pierre-Yves Lagrée, Pascal Ray

CNRS - Université Pierre et Marie Curie Paris 6, UMR 7190, Institut Jean Le Rond d'Alembert, F-75252 Paris, France.

Stéphane Popinet

National Institute of Water and Atmospheric Research, PO Box 14-901 Kilbirnie, Wellington, New Zealand

Bingham plastics exhibit complex behaviors, depending on both geometrical and rheological factors, and are difficult to characterize systematically. This is particularly true in the case of transient flows, where solid-like and fluid-like behaviors coexist in an intermittent fashion. The aim of this contribution is to study the slump of Bingham columns under gravity while varying systematically and independently both the geometry of the system and the rheological parameters. To do so, numerical experiments are carried out in two dimensions (2D) with a non-Newtonian Navier-Stokes code, the Gerris flow solver, using a Volume-Of-Fluid approach. We are able to determine the slump height and the spreading of the column after motion ceased. These characteristics are related to the rheological properties and initial shape through scaling relationships. The results are compared with previous scalings and prediction from the literature. A discussion ensues on the importance of the normalization choice and of unambiguous discrimination between geometrical and material factors.

1 Introduction

The flow of yield stress materials under gravity is encountered in many situations of industrial, engineering and geophysical relevance. Muds and slurries, as those dealt with in off-shore construction, but also in mining processes and in the agro- and food- industries (fertilizers, emulsified food etc), show a typical yield behavior: a minimum stress must be applied for the material to start flowing. Fresh concrete, whose rheological properties are crucial for those using it, is a well-known example of yield stress material (Ferraris & de Larrard, 1998; Schowalter & Christensen, 1998; Roussel et al, 2005). In a different context, lahars resulting from heavy rainfalls in volcanic areas show similar flow properties (Whipple, 1997; Tallarico & Dragoni, 2000). The slow failure of muddy soils is another dramatic manifestation of yield behavior.

Despite their apparent diversity, in a first approximation, all these materials can be described as Bingham plastics in a large number of situations: they behave like solids at low stress, and flow like viscous fluids at high stress. In this simplified picture, a yield stress and a viscosity define them nearly completely. However, in the face of the simplicity of the mathematical form of Bingham's model, Bingham plastics exhibit a complex behavior difficult to characterize systematically. This is particularly true in the case of transient flows, where solid-like and fluid-like behaviors coexist in an intermittent fashion. Because the existence of a yield stress implies the existence of an intrinsic length scale (given by the ratio of the yield stress to the density times gravity $L_y = \tau_y/\rho g$), the geometry of the system will play a role. In the case of gravity induced flows, the height of the system will command whether the system can flow or not (Roussel & Coussot, 2005). This geometrical constraint is not easy to deal with. In spite of its fundamental role in the subsequent flow (Sader & Davidson, 2005), previous works on slump test for concrete do not offer an unambigous characterization of the role of rheology and geometry independently one from the other (Pashias et al, 1996; Ferraris & de Larrard, 1998; Schowalter & Christensen, 1998; Roussel & Coussot, 2005). Extensive theoretical work on the slumping of viscoplastic material was achieved, however it is mostly valid in the framework of long-wave approximation, that is for squat systems (Balmforth et al, 2007; Dusbash et al, 2009; Hogg & Matson, 2009). Predictions using limit analysis for cylinders and rectangles of yield stress material can be made for incipient failure conditions (Chamberlain et al, 2004). Yet, the complex interplay of geometry and rheology in the gravity flow of Bingham systems still needs clarification. Because high values of the yield stress implies small lateral deformation, it is often assumed that plastic viscosity plays no role in the final shape of the slumping system (Sader & Davidson, 2005; Roussel & Coussot, 2005). In the case of low yield stress however, lateral spreading becomes important, hence shear deformation, and viscous stresses is likely to affect the overall deformation. Again, the specific role of the plastic viscosity may depend on the initial geometry of the system.

The aim of this contribution is to study the slump of 2D Bingham columns under gravity while varying systematically and independently both the initial geometry of the system and the two rheological parameters: yield stress and plastic viscosity. To do so, numerical experiments are carried out in two dimensions (2D) with a non-Newtonian Navier-Stokes code, the Gerris flow solver, using a Volume-Of-Fluid approach (Popinet, 2003; Sader & Davidson, 2005; Lagrée et al, 2011). Determining the slump height and the spreading of the column after motion ceased, we relate these characteristics to rheological properties and initial shape and try to disclose "universal" scaling relationships. The results are compared with previous scaling and prediction from the litterature (Sader & Davidson, 2005; Pashias et al, 1996). A discussion ensues on the importance of the normalization choice and the importance of unambiguous discrimination between geometrical and material factors.

2 Numerical model and simulations

The slumping test consists of allowing a column of material to collapse and spread under gravity onto a horizontal plane, as shown in Figure 15 (half-column shown with a symmetry condition). This well-constrained system in terms of both rheology and geometry is of academic interest, and furthermore, is of practical relevance to *in-situ* rheological tests for concrete (the Abrams cone test, for instance) or for the failure of geological material. In practical applications - for instance when testing fresh concrete using slumping tests - the

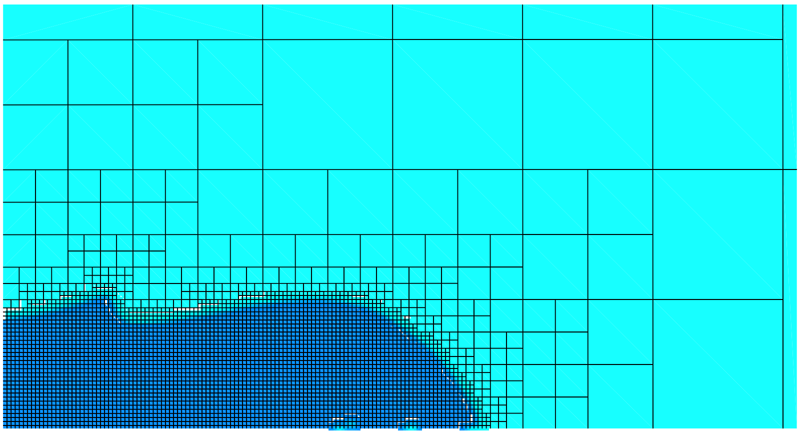

Figure 1: Adaptative mesh refinement during the simulation of a slump using the Gerris flow solver.

column obeys an axisymmetric geometry; for the sake of simplicity however, we consider in the present study a real 2D geometry, but will nevertheless refer to the lateral dimension of the system as *radius*.

2.1 The Gerris flow solver: a two-phase description

The simulations were performed using the (open source) Gerris flow solver in two dimensions. Gerris solves the Navier-Stokes equation for a bi-phasic mixture using a Volume-Of-Fluid approach (Scardovelli & Zaleski, 1999; Popinet, 2003). The existence of two fluids translates numerically in different properties (viscosity and density) on the simulation grid following the advection of the volume fraction representing the proportion of each fluid. In our case, one fluid stands for Bingham plastic (characterized by a yield stress and a plastic viscosity) and the other stands for the surrounding air (with a low density and low viscosity); the position of the interface between the two is solved in the course of time based on the spatial distribution of their volume fraction. This method is in its main features identical to that applied by Davidson et al (2000) and Sader & Davidson (2005) for the gravity flow of visco-plastic material.

In Lagrée et al (2011), we show that choosing for the surrounding fluid (or "air") a viscosity and a density 100 times smaller than that of the non-Newtonian fluid studied does not affect the dynamics of the latter, based on systematic comparison with an analytical solution. Accordingly, in this contribution, we choose for the surrounding fluid a viscosity and a density 100 times smaller than that of the Bingham fluid. The viscosity of the Bingham fluid is constant at large shear and diverges at low shear. Using a simple regularization technics, we implement the viscosity as follows:

$$\eta_{Bingham} = \min\left(\frac{\tau_y}{D_2} + \eta\ ;\ \eta_{max}\right),$$

where τ_y is the yield stress, η is the plastic viscosity and D_2 is given by the second invariant of the strain rate tensor $\boldsymbol{D}$: $D_2 = \sqrt{2D_{ij}D_{ij}}$. Numerically, the divergence of the viscosity is bounded by a maximum value η_{max} set to 10^4 to 10^5 times the value of η; we have checked that the choice of η_{max} does not affect the results as long as η_{max}/η is large enough (down to 10^2 in the configuration studied here). Following this formulation, we see that the plastic viscosity η plays a role only in the limit of sufficiently high deformation; for large values of the yield stress τ_y, its influence is expected to become marginal, justifying the choice of setting its value to zero (Sader & Davidson, 2005; Roussel & Coussot, 2005) or ignoring its influence (Pashias et al, 1996; Schowalter & Christensen, 1998). In this contribution however, we show that the influence of the plastic viscosity η in the sideways spreading, when the latter occurs, is always apparent.

A no-slip boundary condition is imposed at the base of the flow, and a symmetry condition is imposed at the left wall. The Gerris flow solver uses an adaptive mesh refinement as shown in Figure 14, thus limiting computational costs. No experimental data were available to test the results of the numerical simulations of Bingham fluid; however, it was successfully tested against analytical solution for cylindrical Couette flow (Bird et al, 1987) as part of the Gerris test suite [1]. Moreover, the Gerris solver was used to reproduce the gravity flows of granular media as non-Newtonian viscous fluid, and led to the successful recovery of experimental results in different configurations, including the silo (Staron et al, 2012), and more relevantly to the present work, the collapse of 2D columns under gravity (Lagrée et al, 2011). The reader is refered to Popinet (2003, 2009) for a comprehensive presentation of the Gerris Navier-Stokes solver.

[1] `http://gerris.dalembert.upmc.fr/gerris/tests/tests/couette.html`

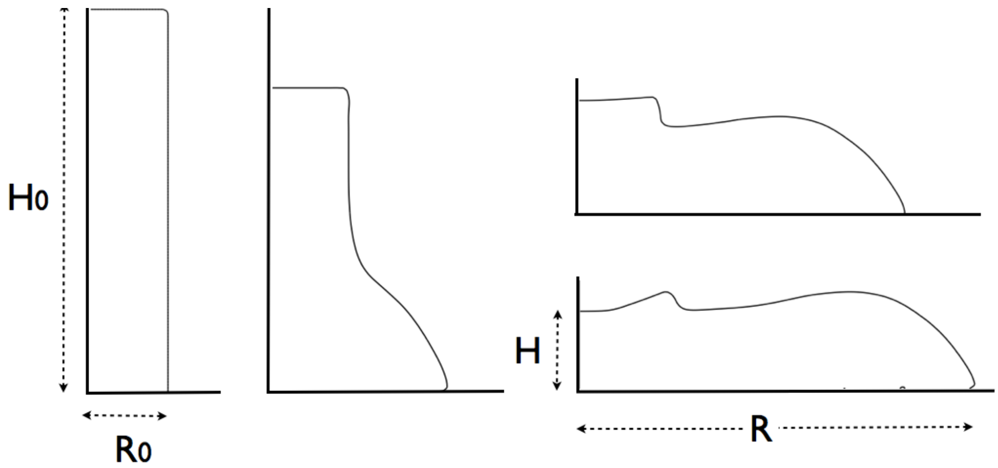

Figure 2: Snapshots of the slumping of a half-column of Bingham plastic simulated with Gerris, with initial aspect ratio $a = H_0/R_0 = 5$, yield stress $\tau_y/\rho g R_0 = 0.33$ and plastic viscosity $\eta/\rho g^{1/2} R_0^{3/2} = 0.86$, at times $t/\sqrt{H_0/g} = 0$, 0.85, 1.70 and in the final state.

2.2 The slumping test: geometrical and rheological parameters

The initial geometry is characterized by the initial (real 2D) radius R_0 and initial height H_0; the initial aspect ratio is denoted $a = H_0/R_0$ (Figure 15). In order to investigate the effect of geometrical factors on the slumping, both the radius R_0 and the initial height H_0 were alternatively varied. Accordingly, the aspect ratio varies between 0.2 and 19.

The final state is characterized by the final spread - or runout - R and the final height H, the slump being defined as the difference between the initial and the final height $H_0 - H$. In the course of time, the position of the front is denoted r and the position of the top of the collapsing column in contact with the left boundary is denoted h. In practice, r and R are given by the maximum lateral excursion of the domain occupied by Bingham material, and h and H by the maximum excursion of the Bingham material at the left-hand-side boundary of the simulation domain. The transition between the Bingham material and the surrounding air being sharp (over 2 to 3 cells), the error when evaluating R and H is about 2% to 5% (error bars are not shown on the graphs).

The rheological properties of the material were systematically varied. Because the initial height H_0 sets the value of the initial compressional stress, to be compared with the char-

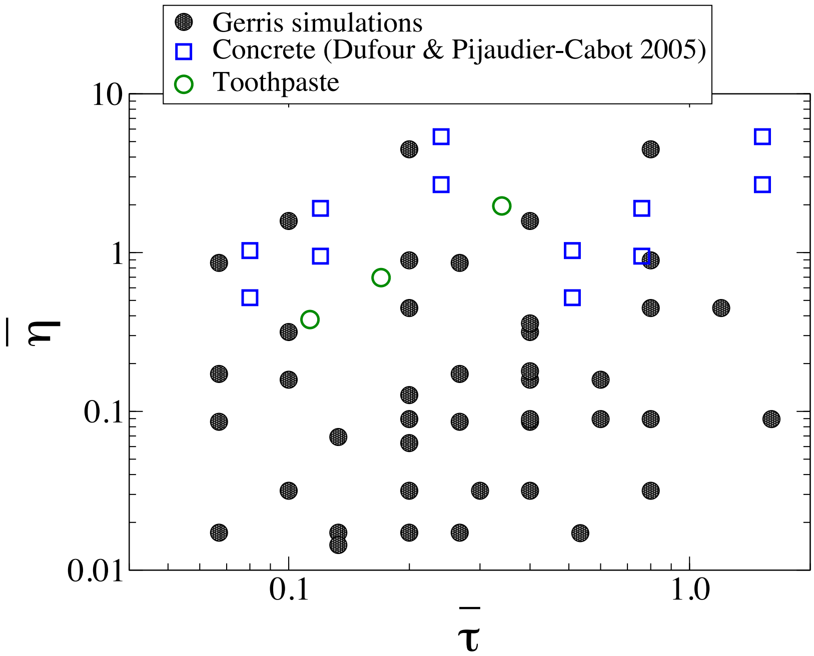

Figure 3: Combined values of the normalized yield stress $\bar{\tau}_y = \tau_y/(\rho g R_0)$ and normalized plastic viscosity $\bar{\eta}_y = \eta_y/(\rho g^{1/2} R_0^{3/2})$ used in the simulations (black circles); each point coincide with a series of simulations with varying aspect ratio a ($0.2 \leq a \leq 19$). Squares and empty circles coincide with values for concrete and toothpaste respectively after proper normalization.

acteristic yield length scale $L_y = \tau_y/\rho g$, we choose to use the initial width R_0 to normalize the rheological parameters in order to allow unambigous discrimination between material and geometrical factors. The effect of the initial height H_0 is singled out using the purely geometrical parameter $a = H_0/R_0$.

The yield stress τ_y was set so that the normalized yield stress $\bar{\tau}_y = \tau_y/\rho g R_0$ varies between 0.06 and 1.6. Since $a = H_0/R_0$ varies between 0.2 and 19, the simulations cover the two following cases: $H_0/L_y << 1$, for which we expect no or little motion to occur, and $H_0/L_y >> 1$, for which large motion is expected. The value of the plastic viscosity η was set so that $\bar{\eta} = \eta/\rho g^{1/2} R_0^{3/2}$ varies between 10^{-2} and 5. Figure 16 shows all the combined values of normalized yield stress and plastic viscosity used for this study; each point on the graph corresponds to a series of simulations with aspect ratio a varying from 0.2 to 19. For comparison, fresh concrete exhibits a yield stress ranging typically from 0.012 to $0.076 \times \rho g L$, and a plastic viscosity typically between 3.10^{-2} and $6.10^{-2} \times \rho g^{1/2} L^{3/2}$, where $\rho \simeq 2500$ kg.m^{-3}, $g = 9.81$ m.s^{-2} and $L = 1$m (data taken from Dufour & Pijaudier-Cabot (2005)). For toothpaste, a typical value for the yield stress is $0.017 \times \rho g L$, while the viscosity is about $0.022 \times \rho g^{1/2} L^{3/2}$ (with $\rho \simeq 1200$ kg.m^{-3}, $g = 9.81$ m.s^{-2} and $L = 1$m). These values, properly normalized using the different values of the initial radius R_0 of the columns, are also shown in Figure 16.

Defining the Bingham number $Bi = \bar{\tau}_y/\bar{\eta}$, Bi ranges from 0.014 to 30 for the total of 1020 simulations performed. Their behavior is analyzed in the following.

3 A typical slump in the course of time

Figure 15 shows different snapshots of the evolution of a column of initial aspect ratio $a = 5$ with plastic viscosity $\eta/\rho g^{1/2} R_0^{3/2} = 0.86$ and yield stress $\tau_y/\rho g R_0 = 0.33$. The corresponding time evolution of the position of the front in the course of time $r(t) - R_0$ and of the slump $H_0 - h(t)$ (normalized by R_0), are displayed in Figure 17. During the flow, the upper-right edge of the column is preserved (due to locally low compressional stress); in the case of very large a, it can be advected downstream. Closer inspection of the

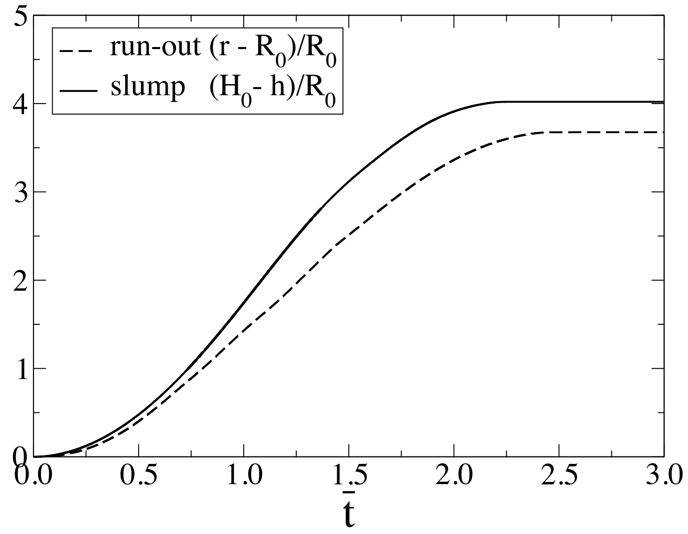

Figure 4: Evolution of the normalized position of the front $(r - R_0)/R_0$ (or run-out) and of the top of the column $(H_0 - h)/R_0$ (or slump) as a function of the normalized time $\bar{t} = t/\sqrt{H_0/g}$ for the system displayed in Figure 15.

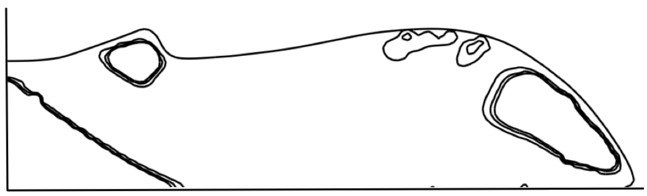

Figure 5: Snapshot showing areas of maximum viscosity close to flow arrest.

state of the spreading layer reveals the existence of areas of higher viscosities (Figure 18): a "dead" corner is located at the basis of the initial column, and spreads sideways while the flow decelerates and stops; small patches of higher viscosity also appear at the surface of the spreading layer. The preserved edge forms one of them. The inner deformations are made visible in Figure 19 by mean of passive tracers; we observe maximum stretching in the vicinity of the bottom and in the inner part of the column.

As expected, the typical evolution described above is sensitive to both the rheological parameters and the initial aspect ratio. Larger values of the plastic viscosity η induce smaller run-outs but larger flow durations due to the increase of the time scale related to viscous deformation. Through a different mechanism, larger values of the yield stress induce smaller run-outs and smaller slumping times, the material being quickly frozen in a stress state below the yielding value. Finally, a dependence on the initial aspect ratio a, rather than on H_0 or R_0 alone, is observed, as previously stressed in Sader & Davidson (2005). In particular, for a small initial aspect ratio, depending on the value of the yield stress, no flow may occur at all. All these points are investigated in details in the following section.

4 Scaling laws for the slumping and spreading

In the analysis of slumping experiments, it is common practice to use the initial height of the system (H_0) as characteristic length scale against which all other quantities are normalized (Pashias et al, 1996; Schowalter & Christensen, 1998; Davidson et al, 2000; Piau, 2005; Roussel & Coussot, 2005). However, the initial height is not the only length scale affecting the deformation of the column: as demonstrated in Sader & Davidson (2005), its initial radius R_0 plays a major role. The initial height sets the value of the initial compressional stress, to be compared with the typical length scale related to the yield stress: $L_y = \tau_y/\rho g$. To single out these two aspects, and prompted by earlier works on slumping of granular matter (Lube et al, 2004; Lajeunesse et al, 2004; Balmforth & Kerswell, 2004; Zenit, 2005; Staron & Hinch, 2005), we will use the initial radius R_0 (rather than the initial height H_0) to normalize the slumping and the spreading of the

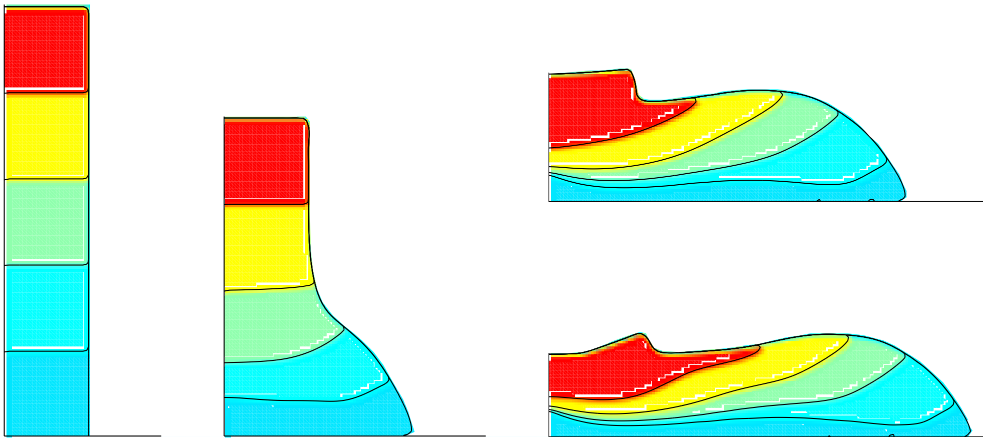

Figure 6: Snapshots of the slumping shown in Figure 15 ($a = 5$, $\tau_y/\rho g R_0 = 0.33$ and $\eta/\rho g^{1/2} R_0^{3/2} = 0.86$), at $t/\sqrt{H_0/g} = 0$, 0.85, 1.70, and in the final state, showing inner deformations using VOF tracers. (color online)

column. Hence, we search for scalings laws relating $(R - R_0)/R_0$ and $(H_0 - H)/R_0$ to $\bar{\tau}_y = \tau_y/\rho g R_0$ and $\bar{\eta} = \eta/\rho g^{1/2} {R_0}^{3/2}$, and to the aspect ratio a.

4.1 A simple prediction based on equilibrium shape

A simple prediction for the final shape of the slumping material can be obtained by assuming that the final state results from the equilibrium between the pressure induced by the variations of the deposit height and the yield stress (Pashias et al, 1996; Roussel et al, 2005; Roussel & Coussot, 2005):

$$\rho g h(r) \frac{\partial h(r)}{\partial r} = \tau_y, \tag{1}$$

and by supposing moreover that the final shape can be approximated by a cone (or triangle in 2D):

$$h(r) \simeq \frac{H}{R}(R - r).$$

Integrating (1) between 0 and R gives immediately:

$$\tau_y = 2\rho g \frac{H^2}{R}. \tag{2}$$

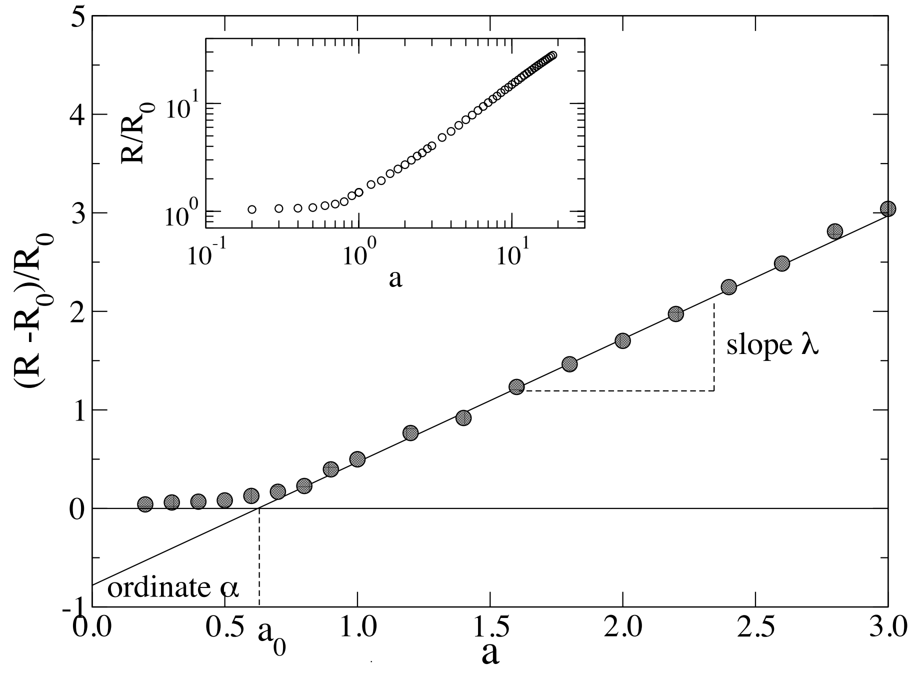

Figure 7: Typical dependence of the normalized runout $(R - R_0)/R_0$ on the initial aspect ratio $a = H_0/R_0$, for $\eta/\rho g^{1/2} R_0^{3/2} = 0.86$ and $\tau_y/\rho g R_0 = 0.33$. Inset: R/R_0 as a function of a in log-log scale.

Since volume conservation implies $HR = 2H_0R_0$, relation (2) leads to the straightforwards predictions:

$$\frac{R}{R_0} = 2 \left(\frac{\rho g R_0}{\tau_y}\right)^{\frac{1}{3}} \left(\frac{H_0}{R_0}\right)^{\frac{2}{3}} = 2\ \bar{\tau}_y^{\,-\frac{1}{3}} \left(\frac{H_0}{R_0}\right)^{\frac{2}{3}}, \tag{3}$$

$$\frac{H}{R_0} = \left(\frac{\tau_y}{\rho g R_0}\right)^{\frac{1}{3}} \left(\frac{H_0}{R_0}\right)^{\frac{1}{3}} = \bar{\tau}_y^{\,\frac{1}{3}} \left(\frac{H_0}{R_0}\right)^{\frac{1}{3}}, \tag{4}$$

with $\bar{\tau}_y = \tau_y/\rho g R_0$. For large values of the aspect ratio a, the approximation of a cone-shape deformation becomes questionable. Moreover, for small values of the yield stress and large aspect ratios, important spreading and large shear deformations will occur, thus large viscous stresses. We can thus suspect these predictions to be inaccurate in this limit. As a matter of fact, both predictions are poorly supported by the result of the simulations, presented in the next section.

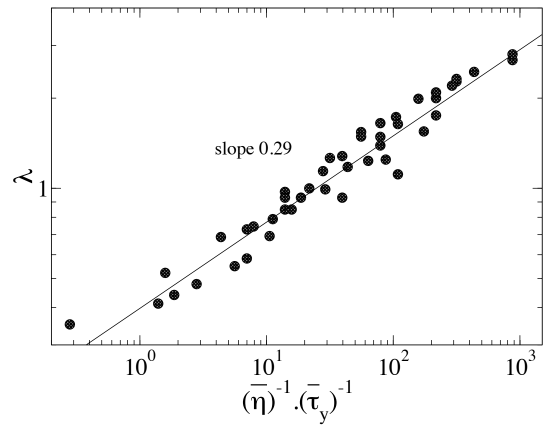

Figure 8: Scaling laws for the runout coefficient λ as a function of the normalized yield stress $\bar{\tau}_y$ and plastic viscosity $\bar{\eta}$.

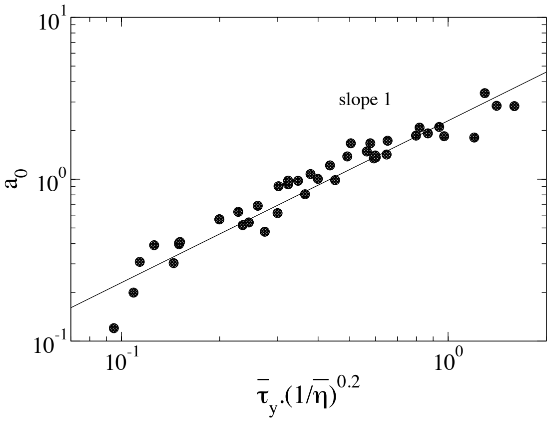

Figure 9: Scaling laws for the critical aspect ratio a_0 (see equation (6)) as a function of the normalized yield stress $\bar{\tau}_y$ and plastic viscosity $\bar{\eta}$.

4.2 Scaling law for the run-out as derived from the simulations

An example of the typical dependence of the normalized runout $(R - R_0)/R_0$ on the initial aspect ratio $a = H_0/R_0$ is displayed in Figure 20. For small values of a, the stress state remains below the threshold: no flow occurs and $(R - R_0)/R_0 = 0$. For larger values of a, the material spreads and we observe an affine dependence between $(R - R_0)/R_0$ and a:

$$\frac{R - R_0}{R_0} = \lambda a - \alpha. \tag{5}$$

Extrapolating this affine dependence allows us for making an estimate of the minimum aspect ratio a_0 characterizing the transition towards sideways spreading: $a_0 = \alpha/\lambda$. Hence, we search for a scaling law for the runout obeying the shape:

$$\begin{cases} (R - R_0)/R_0 = 0 & \text{if } a < a_0 \ , \\ (R - R_0)/R_0 = \lambda(a - a_0) & \text{if } a \geq a_0 \ . \end{cases} \tag{6}$$

We determine the values of λ and α for all 45 sets of simulations performed, corresponding to different values of $\bar{\eta}$ and $\bar{\tau}_y$. The dependences allowing for the collapse of data following a single master curve are reported in Figure 21 and Figure 22 . The prefactor λ is best approximated by

$$\lambda \simeq 0.40 \left[\frac{1}{\bar{\eta}} \times \frac{1}{\bar{\tau}_y}\right]^{0.29 \pm 0.01}, \tag{7}$$

with a correlation coefficient of 0.97 (and $\bar{\tau}_y = \tau_y/\rho g R_0$ and $\bar{\eta} = \eta/\rho g^{1/2} {R_0}^{3/2}$). We observe that both yield stress and plastic viscosity contribute to the sideways spreading with equal weight. We note that the exponent characterizing the dependence on the yield stress is close to the prediction derived in section 4.1 from mass conservation.

It is interesting to note that the minimum aspect ratio characterizing the transition towards sideways spreading a_0 does not reflect the slumping behavior. Indeed, a_0 shows the following dependence:

$$a_0 \simeq 2.25\ \bar{\tau}_y \left(\frac{1}{\bar{\eta}}\right)^{0.20 \pm 0.03},$$

with a correlation coefficient of 0.96. It is surprising that a_0 should depend on the plastic viscosity, moreover following an inverse correlation: indeed we expect a small viscosity to favor slumping. Yet consistently, in the range of parameters studied, we observe that a large viscosity associated with a small yield stress (that is, a small Bingham number $B_i = \bar{\tau}_y/\bar{\eta}$) implies a smaller offset in the dependence between run-out and initial aspect ratio. The fact that no sideways spreading is detected does not mean however that no slumping occurs. Indeed, depending on the value of τ_y, a low plastic viscosity may result in squat columns flanks to deform and create a sideways swell, without the base of the column to actually move. In that case however, slumping occurs. Hence, the critical aspect ratio characterizing the transition to slumping must be estimated from the direct evaluation of the final height H.

4.3 Scaling law for the slumping as derived from the simulations

Using the same set of simulations as shown in Figure 20, the normalized slump $(H_0 - H)/R_0$ as a function of the initial aspect ratio $a = H_0/R_0$ is shown in Figure 23. For small a, no slump occurs and $(H_0 - H)/R_0 = 0$. For larger a, we observe an affine dependence:

$$\frac{H_0 - H}{R_0} = \lambda' a - \alpha', \tag{8}$$

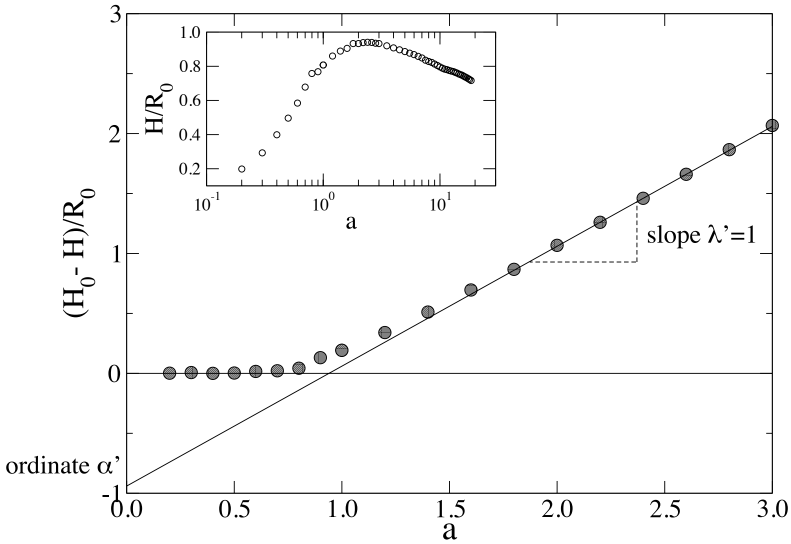

Figure 10: Typical dependence of the normalized slump $(H_0 - H)/R_0$ as a function of the initial aspect ratio $a = H_0/R_0$, for $\eta/\rho g^{1/2} R_0^{3/2} = 0.86$ and $\tau_y/\rho g R_0 = 0.33$. Inset: the normalized final height H/R_0 as a function of a in linear-log scale.

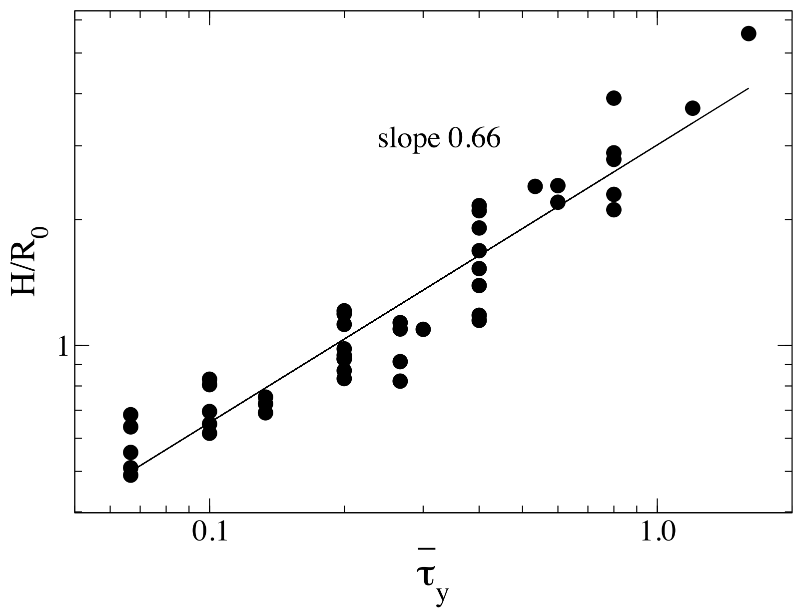

Figure 11: Scaling law for the final normalized height H/H_0 as a function of the normalized yield stress $\bar{\tau}_y = \tau_y/\rho g R_0$.

as exhibited by the run-out (see equation (5)). However in this case, seemingly irrespective of the value of $\bar{\eta}$ or $\bar{\tau}_y$, the slope is constant and equal to one: $\lambda' \simeq 1$. In other words, the effect of the initial aspect ratio a on the final height H is negligible. Hence, relation (8) is equivalent to

$$\frac{H}{R_0} \simeq \alpha' \tag{9}$$

As precedentely, α' is determined for all 45 sets of simulations corresponding to different values of $\bar{\tau}_y$ and $\bar{\eta}$ (shown in Figure 16). The resulting dependence is reported in Figure 24, and is best approximated by:

$$\frac{H}{R_0} \simeq 3.01 \left(\frac{\tau_y}{\rho g R_0}\right)^{0.66\pm0.03} = 3.01\; \bar{\tau}_y^{\;0.66\pm0.03} \tag{10}$$

with a correlation coefficient of 0.95. The final height of the collapsed column is thus independent of the initial height, presumably due to the absence of large inertial effects. Moreover, it is not affected by the value of the plastic viscosity $\bar{\eta}$, as generally assumed in numerical studies (Tattersall & Banfill, 1983; Schowalter & Christensen, 1998; Sader & Davidson, 2005; Roussel & Coussot, 2005) and theoretical derivations (Chamberlain et al, 2004)

Using (8) and (10), we can write:

$$\begin{cases} (H_0 - H)/R_0 = 0 & \text{if } a < a_c \;, \\ (H_0 - H)/R_0 = (a - a_c) & \text{if } a \geq a_c \;, \\ a_c = 3.01\; \bar{\tau}_y^{\,0.66}, & \end{cases} \tag{11}$$

where a_c is the critical aspect ratio characterizing the transition to slumping.

This result is qualitatively in agreement with the result of Sader & Davidson (2005) where a polynomial relation between $\rho g R_0/(2\tau_y)$ and $1/a_c$ was observed for axisymmetric columns: we find that a polynomial relation (although of a different order) is acceptable for the same range of $\bar{\tau}_y$ (see Figure 25). Differences between the two approaches includes the geometry (axisymmetric in Sader & Davidson (2005) vs planar in the present contribution) and the values of the plastic viscosity (equal to zero in Sader & Davidson (2005) while varied over two orders of magnitude in the present contribution); yet, the dependences found involve the same parameters, namely yield stress and critical aspect ratio, following the same trend.

By contrast, our results are not fully compatible with the theoretical prediction of Pashias et al (1996), also discussed in Schowalter & Christensen (1998); Davidson et al (2000); Roussel & Coussot (2005). Indeed, the theoretical derivation in Pashias et al (1996) leads to the following prediction for the slump:

$$\frac{H_0 - H}{H_0} = 1 - 2\frac{\tau_y}{\rho g H_0}\left(1 - \ln\left(2\frac{\tau_y}{\rho g H_0}\right)\right). \tag{12}$$

Rewritten in term of final height H and normalized according to the choice adopted in the present contribution, (12) is equivalent to:

$$\frac{H}{R_0} = 2\bar{\tau}_y\left(1 - \ln\left(2\bar{\tau}_y a\right)\right), \tag{13}$$

with $\bar{\tau}_y = \tau_y/\rho g R_0$. While our simulations suggest that H/R_0 is only dependent on $\bar{\tau}_y$ (scaling (10)), the prediction of Pashias et al (1996) implies an additional dependence on the aspect ratio a. In other words, it combines the effect of both rheological properties and geometry, i.e. compressional stress. This is illustrated in Figure 26 where we have reported $(H_0 - H)/H_0$ as a function of $\tau_y/\rho g H_0$ for two distinct values of the yield stress τ_y, i.e. corresponding to two different materials. For each value of τ_y (i.e. for each material), the aspect ratio a varies, while R_0 and $\bar{\eta}$ are kept constant. In the case $\tau_y = 0.01\rho g L$ (where $L = 1$m is an arbitrary length scale not related to the system geometry) we observe that our data points nicely match the prediction (13); this is however a purely geometrical effect due to the representation in terms of $\tau_y/\rho g H_0$. Indeed, varying a implies varying H_0 and thus varying the ratio $\tau_y/\rho g H_0$ although τ_y is constant: in this precise case, we verify equation (12) while actually not probing the material property.

If we look at the case $\tau_y = 0.04\rho g L$ (where $L = 1$m), we observe a systematic shift compared to the case $\tau_y = 0.01\rho g L$, that is, our data do not collapse following (12); yet, it is still compatible in shape with equation (12). Here again, only the geometry (i.e. the variations of a) is responsible for the relative agreement with the prediction (12), without involving any meaning in terms of the material rheological properties.

This result prompt a comment on the importance of the normalization choice. By using the initial height, one mixes the effect of compressional stress and rheology. While

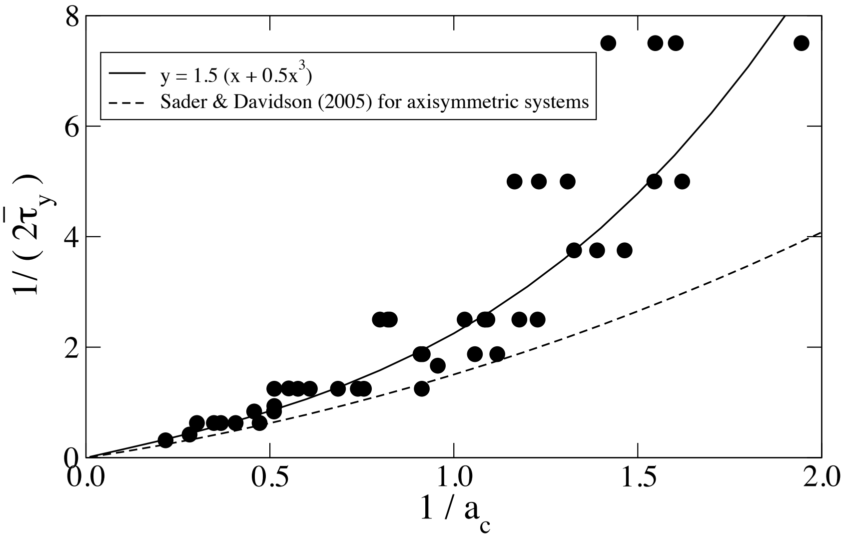

Figure 12: Comparison with the results of Sader & Davidson (2005) for axisymmetric columns with zero viscosity: $1/2\bar{\tau}_y \simeq 1/a_c + 0.5(1/a_c)^2 + 0.005(1/a_c)^4$. We find in 2D $1/2\bar{\tau}_y \simeq 1.5(1/a_c + 0.5(1/a_c)^3)$.

this is common practice to define such non-dimensional numbers where the behavior of the system is well described by an equation (as Newtonian fluids for instance), it is not straightforward when the behavior of the system regarding all independent parameters is far from fully understood, as for the Bingham slump. As a result, one can easily mistake the effect of geometry for those of material, thus allowing for incorrect interpretation. This is particularly likely to happen in experiments where the yield stress of materials used varies over a relatively small interval, while geometry can be changed at command.

5 Discussion

5.1 Comparison with the slumping of granular material

Granular materials and Bingham plastics share an important rheological property: they behave like a solid at low shear stress and like a fluid at higher shear stress. However, the threshold marking the transition between one and the other state is of a different nature. While in Bingham plastics, the threshold is given by an absolute yield value τ_y, the threshold in granular matter is given by frictional properties, and thus depends locally on

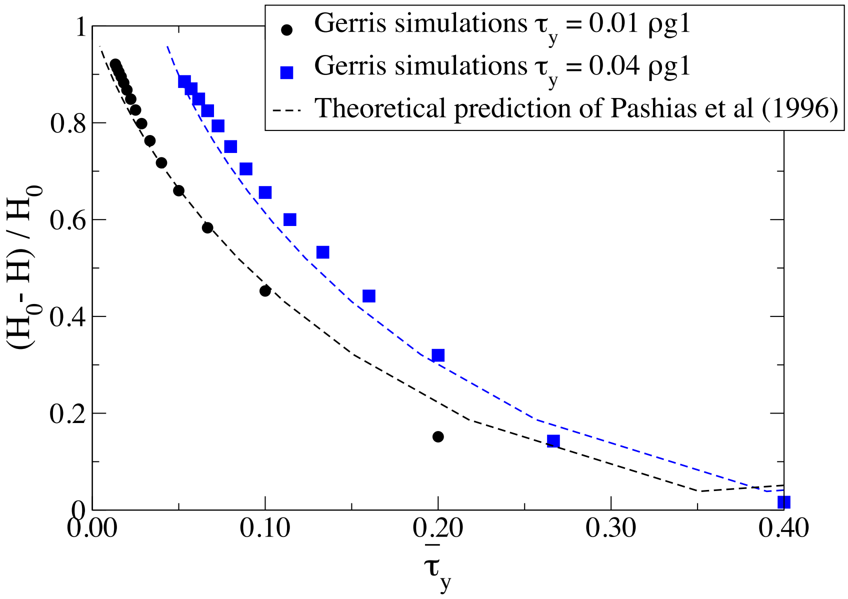

Figure 13: Comparison with the results of Pashias et al (1996): Slump normalized by the initial height $(H_0 - H)/H_0$ as a function of the normalized yield stress $\bar{\tau}_y = \tau_y/\rho g H_0$ for two series of simulations corresponding to two given materials (*ie* two given values of $\tau_y/\rho g L$, $L = 1$m), and theoretical prediction from Pashias et al (1996) (see equation (12)). The agreement reflects geometrical constraints only.

the compressional stress: $\tau_y = \mu P$, where μ is the coefficient of friction and P the pressure. Moreover, granular flows exhibit shear thickening properties. It is interesting to observe how these differences reflect on the slumping dynamics and the corresponding scaling laws. In Lajeunesse et al (2004); Lube et al (2004); Balmforth & Kerswell (2004); Staron & Hinch (2005) for instance, the collapse of granular material was investigated experimentally (using sand, rice, glass beads) and numerically (applying the discrete Contact Dynamics method), following the same set-up as applied in this paper. The scaling laws thus obtained in 2D read:

$$\frac{R - R_0}{R_0} = \lambda(\mu) \times a^{\alpha}, \quad a \geq a_c \tag{14}$$

$$\frac{H}{R_0} = \lambda'(\mu) \times a^{\alpha'}, \quad a \geq a'_c \tag{15}$$

with $\alpha \simeq 0.67$ and $\alpha' \in [0.3, 0.4]$ depending on the authors, and where a_c and a'_c are critical values of the aspect ratio, varying from 0.7 to 2.8 depending on the authors. The prefactors λ and λ' are functions of the coefficient of friction μ only.

The difference between these scalings and those obtained from the present simulations - that is relations (7) and (10) - is manifest. However, they might not be incompatible. Indeed, the yield stress for granular columns is given by $\tau_y = \mu\rho g H_0$. Replacing this in (10) gives immediately $H/R_0 = \lambda'(\mu)\, a^{0.66}$, where $\lambda'(\mu) = 3.01\, \mu^{0.66}$, thus becoming similar in shape to (15). In the same way, replacing $\tau_y = \mu\rho g H_0$ in (7) leads directly to $(R - R_0)/R_0 \propto \lambda(\mu)\, a^{0.71}$, where $\lambda(\mu) = 4.0\, \mu^{-0.29}$ (a trend compatible with numerical observations in Staron & Hinch (2007))), thus sharing similarities with (14).

Viscous terms are more intricate. In dry granular flows, the viscosity can be approximated by $\eta = \mu P/|\dot{\gamma}|$, where $\dot{\gamma}$ is the shear rate (Jop et al, 2006; Lagrée et al, 2011). There are no obvious scales for the pressure and the shear rate during the sideways spreading. Note however that the choice of $P = \rho g R_0$ and $|\dot{\gamma}| = \sqrt{g/R_0}$ leads immediately to the following relation between friction and viscosity: $\mu = \eta/\rho g^{\frac{1}{2}} R_0^{\frac{3}{2}}$, and can thus be replaced in the scaling (7). This is certainly too speculative to draw any conclusion on the viscous behavior of granular slump experiments. But we can nevertheless conclude that Bingham and granular scalings may be less different than they appear at first. Granular matter forms an example of visco-plastic behavior where yield stress and viscosity are not independent, but are coupled (here through internal friction properties). We may question the existence of such coupling in other common materials, like muds or fresh concrete.

5.2 About cement and concrete

Granular matter forms an example of visco-plastic behavior where yield stress and viscosity are coupled. It would be interesting to establish whether such a coupling exists in real Bingham-like materials, and among them concrete. Indeed, unlike the ideal Bingham material simulated in this paper, viscosity and yield stress in fresh concrete are not necessarily independent quantities. For instance, the data given in Dufour & Pijaudier-Cabot (2005) for three different model concretes suggest that plastic viscosity and yield stress are related quantities: the greater the viscosity, the greater the yield stress.
From the systematic analysis of the simulations, the final slump height appears to be essentially independent of the viscosity, but to scale like $(\tau_y/\rho g R_0)^{0.66}$. This brings the conclusion that slumping tests, like the Abram cone widely used to measure the properties of fresh concrete, do give information on the yield stress, but little on the viscosity. Clarifying the relation between these two quantities might contribute to a more reliable calibration of slump tests as in-situ measurements of rheological parameters. In this perspective, the present study suggests that sideways spreading rather than slumping keeps the signature of the viscous behavior.

6 Conclusion

Applying the Gerris Navier-Stokes solver allowing for the modeling of bi-phasic mixtures using a VOF method, we simulate the collapse of columns of Bingham plastics under gravity in 2D. The rheological properties of the material - plastic viscosity and yield stress - as well as the geometry of the columns - initial radius and initial height - were varied independently. The final slumping height and final run-out were measured and scaling laws derived. Our results show that the runout R increases linearly with the initial height of the column H_0, with a prefactor depending inversely on both plastic viscosity and yield stress:

$$\begin{cases} (R-R_0)/R_0 = 0 & \text{if } a < a_0 \ , \\ (R-R_0)/R_0 = \lambda(a-a_0) & \text{if } a \geq a_0 \ , \\ \lambda \simeq 0.40 \left[\frac{1}{\bar\eta} \times \frac{1}{\bar\tau_y}\right]^{0.29\pm0.01}, & \\ a_0 \simeq 2.25 \ \bar\tau_y \left(\frac{1}{\bar\eta}\right)^{0.20}, & \end{cases}$$

where $a = H_0/R_0$ is comprised in the interval $[0.2, 19]$, $\bar\tau_y = \tau_y/\rho g R_0$ is comprised in the interval $[0.06, 1.6]$ and $\bar\eta = \eta/\rho g^{1/2} {R_0}^{3/2}$ is comprised in the interval $[0.01, 5]$.

By contrast, we find that the final height H is essentially insensitive to plastic viscosity and depends on the value of the yield stress. We find no effect of the initial height of the column, whereby we conclude that inertial effects are negligible. We derive the transition to slumping following the scaling:

$$\begin{cases} (H_0-H)/R_0 = 0 & \text{if } a < a_c \ , \\ (H_0-H)/R_0 = (a-a_c) & \text{if } a \geq a_c \ , \\ a_c \simeq 3.01 \, {\bar\tau_y}^{0.66}, & \end{cases}$$

where $a = H_0/R_0$ is comprised in the interval $[0.2, 19]$ and $\bar\tau_y = \tau_y/\rho g R_0$ is comprised in the interval $[0.06, 1.6]$. This last result is compatible with the conclusions of Sader & Davidson (2005) relative to the slump in axisymmetric configuration. When compared with the theoretical prediction of Pashias et al (1996), we find a partial agreement which however only reflects the geometrical constraints imposed by varying the aspect ratio. This result shows the importance of the normalization choice. By using the initial height, one mixes the effect of compressional stress, geometry and rheology in one single non-dimensional parameters. While this is common practice to define such non-dimensional numbers where the behavior of the system is well described by an equation (as Newtonian fluids for instance), it is not straightforward when the behavior of the system regarding all independent parameters is far from fully understood, as for the Bingham slump. As a result, one can easily mistake the effect of geometry for those of the material properties, thus allowing for incorrect interpretation. This is particularly likely to happen in experimental settings where the yield stress of materials used varies over a relatively small interval, while geometry can be changed at command.

The scaling laws discussed in this contribution were obtained for 2D configurations; an interesting step for practical application would be to investigate how the scalings are modified in the axisymmetric case, as studied by Sader & Davidson (2005). This aspect will be addressed in future work.

References

Balmforth, N.J. and Kerswell, R.R.: Granular collapse in two dimensions. J. Fluid Mech. **538**, 399428 (2004)

Balmforth, N. J., Craster, R. V., Peronac, P., Rustd, A.C. and R. Sassie Viscoplastic dam breaks and the Bostwick consistometer, Journal of Non-Newtonian Fluid Mechanics Volume **142**,13, p. 6378 (2007).

Bird, R. B., Armstrong, R. C. and O. Hassager. Dynamics of polymeric liquids. Wiley-Interscience, second edition edition (1987).

Chamberlain, J. A., Horrobin, D. J., Landman, K. A. and Sader, J. E, Upper and lower bounds for incipient failure in a body under gravitational loading, J. Applied Mech **71**, 586-589 (2004).

Davidson M. R, Khan N. H & Yeow, Y. L., Collapse of a cylinder of a Bingham fluid, ANZIAM J. **42**(E), pp C499-C517 (2000)

Dubash, N., Balmforth, N. J., Slima, A. C. & S. Cochard, What is the final shape of a viscoplastic slump?, Journal of Non-Newtonian Fluid Mechanics, **158**(13), p. 91-100 (2009).

Dufour, F. & Pijaudier-Cabot, G. Numerical modelling of concrete flow: homogeneous approach, Int. J. Numer. Anal. Meth. Geomech., **29** 4, pages 395416 (2005).

Ferraris, C. F. and de Larrard, F., Modified Slump Test to Mea-sure Rheological Parameters of Fresh Concrete, *Cement, Concrete and Aggregates*, **20** (2), pp. 241-247 (1998).

Hogg, A. J. & Matson, G. P. , Slumps of viscoplastic fluids on slopes, Journal of Non-Newtonian Fluid Mechanics, **158**, Issues 13, p.101112 (2009).

Jop, P., Forterre, Y. & Pouliquen, O., A rheology for dense granular flows. Nature **441**, 727730 (2006).

Lagrée, P.-Y., Staron, L. & Popinet, S., The granular column collapse as a continuum: validity of a two-dimensional NavierStokes model with a $\mu(I)$-rheology, *J. Fluid Mech.*, **686**, pp 378-408 (2011).

Lajeunesse, E., Mangeney-Castelneau, A. & Vilotte, J.-P., Spreading of a granular mass on an horizontal plane. Phys. Fluids **16**, 23712381 (2004).

Lube, G., Huppert, H. E., Sparks, R. S. J. & Hallworth, M. A. , Axisymmetric collapses of granular columns. J. Fluid Mech. **508**, 175199 (2004).

Pashias, N., Boger, D. V., Summers, J. & Glenister, D. J., A fifty cent rheometer for yield stress measurement, J. Rheol. **40**(6), 1179 (1996).

Piau, J.-M., Axisymmetric slump and spreading of cohesive plastic soft materials: a yield stress measurement by consisto-rheometry, J. Rheol. **49**, 1253 (2005).

Popinet, S., Gerris: a tree-based adaptive solver for the incompressible Euler equations in complex geometries. J. Comput. Phys. **190** (2), 572600 (2003).

Popinet, S., An accurate adaptive solver for surface-tension-driven interfacial flows. J. Comput. Phys. **228**, 58385866 (2009).

Roussel, N., Stefani, C, and Leroy, R., From mini-cone test to Abrams cone test: measurement of cement-based materials yield stress using slump tests, Cement and Concrete Research, **35** 5, 817822 (2005).

Roussel, N. & Coussot, P., "Fifty-cent rheometer" for yield stress measurements: from slump to spreading flow, J. Rheol. **49**, 705 (2005).

Sader, J. E. & Davidson, M. R., Scaling behavior for gravity induced flow of a yield stress material, J. Rheol. **49**, 105 (2005).

Scardovelli, R. & Zaleski, S. Direct numerical simulation of free-surface and interfacial flow Annu. Rev. Fluid Mech. **31**, 567-603 (1999)

Schowalter, W. R. and Christensen, G., Toward a rationalization of the slump test for fresh concrete: Comparisons of calculations and experiments, J. Rheol. **42**, 865 (1998).

Staron, L. & Hinch E. J., Study of the collapse of granular columns using 2D discrete-grains simulation, *J. Fluid Mech.*, **545**, pp 1-27 (2005).

Staron, L. & Hinch E. J., The spreading of a granular mass: role of grain properties and initial conditions, Granular Matter, **9**, p205-217 (2007).

Staron, L., Lagrée, P.-Y. & Popinet, S., The granular silo as a continuum plastic flow: The hour-glass vs the clepsydra, Phys. Fluids **24**(10), 113303, doi:10.1063/1.4757390 (2012)

Tallarico, A. and Dragoni, M., A three-dimensional Bingham model for channeled lava flows, J. Geophys. Res., **105**, B11 (2000).

Tattersall, G. H. & Banfill, P. G. F, The rheology of fresh concrete, Pitman Advanced Pub. Program (1983)

Vola, D., Babik, F. and Latché, J.-C., On a numerical strategy to compute gravity currents of non-Newtonian fluids, *Journal of Computational Physics*, **201** Issue 2, pp 397-420 (2004).

Whipple, K. X., Open-Channel Flow of Bingham Fluids: Applications in Debris-Flow Research, The Journal of Geology, **105** (2), pp. 243-262 (1997).

Zenit, R., Computer simulations of the collapse of a granular column, Phys. Fluid **17**, 031703 (2005)